


Ultra-Short Pulses With High Repetition Frequency in Transmission Plasmonic Systems

Shilei Li , Yanan Qi, Liming Li, Dan Yu, and Benyi Wang

Abstract—Ultra-short pulses with high repetition frequency have great application prospects in the field of nano-optics. Here, in the case of continuous wave incidence, the femtosecond pulses with THz repetition frequency are achieved in the transmission system consisting of quantum emitters (QEs) and plasmonic resonators. The generation mechanism of the ultra-short pulses with high repetition frequency is elucidated by semi-classical model. Attribute to the presence of the two-level QEs, the field amplitude in plasmonic resonator is oscillating with time, resulting in the transmittance of the system behave as the form of pulse oscillation. Moreover, the pulse repetition frequency and extinction ratio can be freely controlled by the incident light intensity and QEs number density to obtain the required ultra-short pulses at nanoscale. This also has potential applications in high-speed signal processing fields and generating optical clock signals that can be used in optical computing.

Index Terms—Femtosecond pulses, THz repetition frequency, plasmonic resonator, quantum emitters.

I. INTRODUCTION

RESEARCH on nanolasers has made great progress since Bergman and Stockman proposed the concept of spaser (Surface Plasmon Amplification by Stimulated Emission of Radiation) in 2003 [1], [2], [3], [4]. However, achieving ultra-short pulses with high repetition frequency is still one of the main topics to be investigated and resolved urgently in the field of nano-integrated optics. Photonic crystal (PC) nanolasers operating under electrical injection inevitably introduced both scattering and absorption losses, which also has complications of poor heat conduction and low mechanical stability [5], [6]. The miniaturization of semiconductor nanowire lasers is limited by the diffraction limit, so it is extremely difficult to further reduce the resonator size [4]. Many studies show that metal-based nanostructures become the key ingredient to solve this problem [7], [8], [9]. Because of they have ability to break the diffraction limit [10], and the light can also be localized to the nanoscale, thereby enhancing the interaction between light and quantum emitters (QEs) [11], [12]. And the investigations on

the coupling between metal-based nanostructures and QEs also indicate that the hybrid system of plasmonic resonator and QEs is very competitive for obtaining ultra-short pulses with high repetition frequency at the nanoscale.

Meanwhile, the interaction between light and QEs is studied deeply and comprehensively in recent years [13], [14], [15], [16], and the strong coupling between metallic nanostructures and QEs has been experimentally realized [17], [18]. The ultrafast Rabi oscillations between excitons and plasmons were also observed in metal nanostructures with J-aggregates [19]. Whereafter, Demetriadou et al. investigated the spatiotemporal dynamics and control of strong coupling in plasmonic nanocavities [20]. Liu and Ren et al. studied the strong interaction between light and QEs in open plasmonic nanocavity systems [21], [22], and very significant Rabi splitting were observed at room temperature. These investigations laid the foundation for the interaction between light and QEs to be applied in nano-integrated optics. And we find that the coupling between plasmonic resonators and QEs can also be used to obtain femtosecond pulses with high repetition frequency in the case of continuous wave incidence, which is rarely reported in plasmonic resonator systems. Moreover, traditional methods are unable to satisfy the application requirements of many high-speed signal processing fields at the nanoscale, such as optical communications [23], optical interconnection [24], [25], [26], [27], and on-chip sensing [28], [29], [30], [31]. So, femtosecond pulses with high repetition frequency are highly desirable at nanoscale.

In this paper, we find that the coupling between QEs and plasmonic resonators can also be used to generate femtosecond pulses with THz repetition frequency in the case of a continuous wave input. The transmission response of the hybrid system are numerically and theoretically studied. Under the weak excitation limit, obvious mode splitting appears in the transmission spectrum of the system, which indicates that the coupling between the plasmonic resonators and QEs is prominent. However, when the intensity of the excitation light is relatively strong, the QEs in nanowire will oscillate between the upper and lower energy levels. This means the output power of the QEs is in the form of oscillation, which resulting in the transmittance of the system also oscillate with time in the form of pulse. Moreover, the pulse repetition frequency and extinction ratio can be freely controlled by the incident light intensity and the QEs number density to achieve the required pulse form. This provides a method to obtain ultra-short pulses with high repetition frequency at the nanoscale.

Manuscript received 3 May 2023; revised 17 July 2023; accepted 28 July 2023. Date of publication 1 August 2023; date of current version 14 August 2023. This work was supported in part by the National Natural Science Foundation of China under Grants 12104261, 12104260, 62105188, and 62005146 and in part by the Natural Science Foundation of Shandong Province under Grants ZR2020QA070 and ZR2020QA058. (Corresponding author: Shilei Li.)

The authors are with the School of Physics and Optoelectronic Engineering, Shandong University of Technology, Zibo 255049, China (e-mail: lishilei@sdut.edu.cn).

Digital Object Identifier 10.1109/JPHOT.2023.3300923

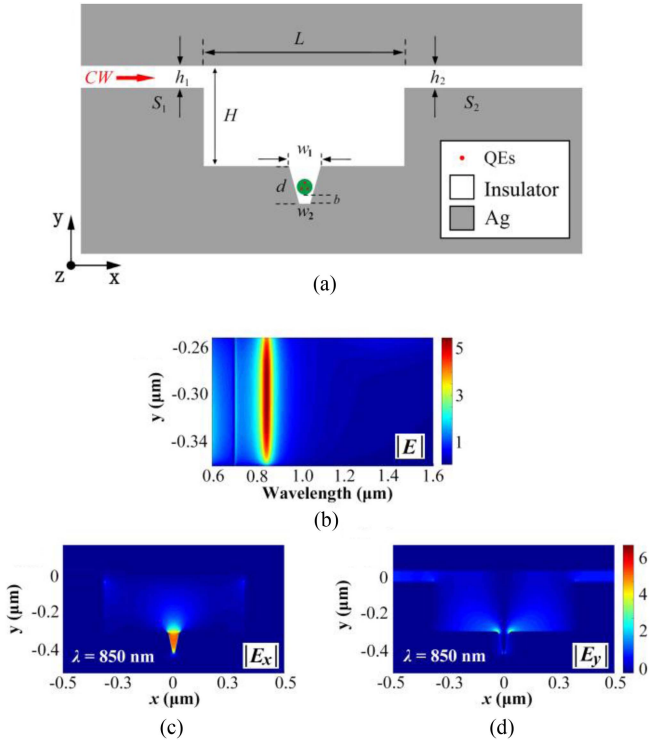


Fig. 1. (a) Schematic diagram of the hybrid system of plasmonic resonator and QEs. The complex dielectric function of the QEs is described by the Lorentz model [33]: $\varepsilon(\omega) = \varepsilon_\infty - f\omega_L^2/(\omega^2 - \omega_L^2 + i\gamma\omega)$. The insulator is set to air with a refractive index of 1. The metal around the VG cavity is silver. The widths of waveguides S_1 and S_2 are $h_1 = 50$ nm and $h_2 = 50$ nm. The length and height of the rectangular cavity are $L = 640$ nm and $H = 280$ nm, respectively. The width and depth of the VG cavity are $w_1 = 50$ nm and $d = 102$ nm, the bottom width is $w_2 = 10$ nm. The diameter of the nanowire is 16 nm, and the distance from its bottom to the bottom of the VG cavity is $b = 34$ nm. (b) Distribution of electric field $|E|$ on center line q (in the left inset of Fig. 1(a)) at different wavelengths. (c) and (d) Distribution of the electric field components $|E_x|$ and $|E_y|$ at the resonant wavelength of 850 nm.

Compared with our previous work [32], a rectangular cavity is added to the plasmonic coupling system in this paper. Due to the presence of the rectangular cavity, not only the effective mode volume of the V-groove (VG) cavity is enormously reduced which could improve the coupling strength between the VG cavity and QEs, but the coupling decay time between the VG cavity and the waveguide is also increased greatly. The improvement of coupling strength and coupling decay time has great advantages in obtaining pulses with high repetition rate, and the required QEs number density is reduced by an order of magnitude. This is very advantageous for preparing corresponding devices in experiments. In addition, some new research content has been added in this paper, such as how to control the duration of pulses and the spectral characteristics of pulses.

II. STRUCTURE AND FIELD DISTRIBUTION

The investigated hybrid system of plasmonic resonator and QEs is shown in Fig. 1, which consists of two waveguides, a rectangular cavity, a V-groove (VG) cavity and a nanowire embedded with two-level QEs. The incident wave is continuous wave (CW) in transverse magnetic (TM) mode, which is input

from the waveguide S_1 on the left. The aim of our investigation is the influences of the incident light intensity and the QEs number density on the transmission response of the hybrid system in the case of continuous wave incidence together with the evolution of the transmittance over time.

In order to obtain stronger coupling between the plasmonic resonator and QEs, the electric field distribution without nanowire in VG cavity is investigated first. Fig. 1(b) shows the pseudo-color image of the electric field distribution on the centerline q of the VG cavity in Fig. 1(a) utilizing two-dimensional FDTD method, the incident light intensity is set to 1. Fig. 1(c) and (d) respectively show the distribution of the electric field components $|E_x|$ and $|E_y|$ in the plasmonic resonator when the incident light wavelength is 850 nm. The electric field energy in plasmonic resonator is mainly concentrated in the VG cavity, the energy in rectangular cavity is close to zero, and the electric field component in VG cavity is mainly $|E_x|$, component $|E_y|$ is almost zero. Therefore, in order to obtain stronger coupling between plasmonic resonator and QEs, the transition dipole moment of the QEs should be as parallel as possible to the x-axis.

III. WEAK EXCITATION LIMIT

Before studying the transmission response of the hybrid system between plasmonic resonator and QEs, it is necessary to investigate the transmission response of the system without nanowire in VG cavity in order to obtain the coupling parameters between the waveguide and the resonant mode in plasmonic resonator. These coupling parameters are necessary for analyzing the evolution of the transmittance with time in Section IV. When the two waveguides are symmetrical about the rectangular cavity and equal in width, according to the multimode interference coupled mode theory (MICMT) [33], the transmission coefficient of the coupled system can be expressed as follows

$$t = \sum_m \frac{2e^{i\varphi_m}}{-i(\omega - \omega_m)\tau_m + 2 + \frac{\tau_m}{\tau_{m0}}} \quad (1)$$

where, ω_m is the resonant angular frequency of the m -th mode of the plasmonic resonator. τ_m is the coupling decay time between the waveguide and the m -th resonant mode, τ_{m0} is the decay time of the internal loss. φ_m is the total phase difference between the waveguide and the m -th resonant mode. The transmittance of the coupled system is $T = |t|^2$.

It is well known that there are many resonant modes in plasmonic resonator. In order to facilitate theoretical analysis, the transmission coefficient of each mode is set to be $t_m = 2e^{i\varphi_m}/[-i(\omega - \omega_m)\tau_m + 2 + \tau_m/\tau_{m0}]$. Here, we only consider two resonant modes that have great impact on the transmission coefficient of the system. One of them is the resonant mode in the VG cavity (the distribution of the electric field component has been shown in Fig. 1(c) and (d)), which could be called TM_v mode (the field is represented by a_1) and the resonant wavelength is 850 nm. Another resonant mode is the $TM_{1,0}$ mode (the field is represented by a_2) in the rectangular cavity, of which the resonant wavelength is 1390 nm and the field distributions of $|E_x|$ and $|E_y|$ are given by Fig. 2(a) and (b). It can be seen from Fig. 2(a) and (b) that the electric field component

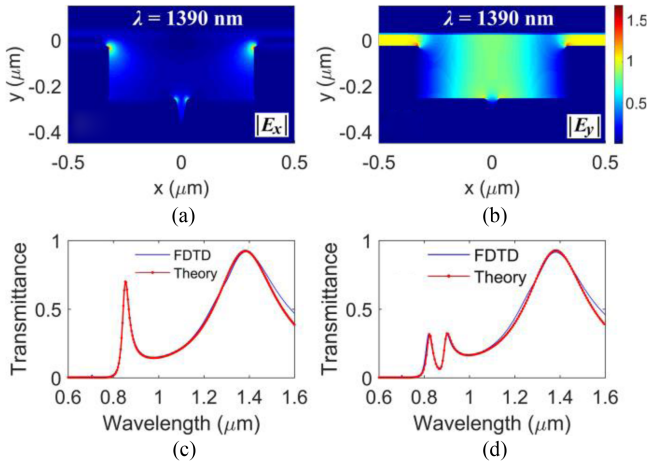


Fig. 2. (a) and (b) The distribution of the electric field components $|E_x|$ and $|E_y|$ at the resonant wavelength of 1390 nm. (c) The simulation (blue) and theoretical (red) curves of the transmittance of the coupled system without nanowire in VG cavity. The fitting parameters are $\tau_1 = 56$ fs, $\tau_2 = 13$ fs, $\tau_{10} = 100$ fs, $\tau_{20} = 120$ fs, $\varphi_1 = 0.4\pi$, $\varphi_2 = -0.5\pi$, respectively. (d) The simulation (blue) and theoretical (red) curves of the transmittance of the hybrid system with nanowire in VG cavity. Here, the lorentz model parameters of the nanowire are $\varepsilon_\infty = 1.4$, $f = 0.4$, $\omega_L = 2.10 \times 10^{15}$ rad/s, $\gamma = 3.85 \times 10^{13}$ rad/s, respectively. The coupling strength is $g_1 = 9 \times 10^{13}$ rad/s. Since the nanowire is placed in VG cavity, the coupling decay time of the TM_v mode slightly changes to $\tau_1 = 50$ fs, while other fitting parameters remain unchanged.

of the $TM_{1,0}$ mode in rectangular cavity is mainly $|E_y|$, and the component $|E_x|$ is almost zero. In the range of 600 nm \sim 1600 nm, the transmission response of the system is mainly affected by these two resonant modes. So, the transmittance of the system can be simplified as $T = |t_1 + t_2|^2$. Fig. 2(c) shows the simulation (blue line) and theoretical (red line) results of the transmittance, in which there are two peaks on the transmittance curve. The position of the first peak is at 854 nm which can be adjusted by the depth of the VG cavity [35], but the width has almost no effect on it. The position of the second one is at 1386 nm and can be adjusted by the length of the rectangular cavity, the height has almost no effect on the position of the second peak [35]. The parameters of the coupling system without nanowire in VG cavity can be obtained by fitting the theoretical curve to the simulation curve. But for the hybrid system with the nanowire placed in VG cavity, the coupling parameters are slightly different. Based on the research above, we need to further obtain the coupling parameters of this hybrid system for the investigation in Section IV. So, next investigated will be the transmission response of the hybrid system under the weak excitation limit when there is a nanowire embedded with QEs placed in the VG cavity.

The QEs system can be described by Bloch equation, the dipole transition equation of the system can be expressed as

$$\frac{d\rho_{eg}}{dt} = -(i\omega_A + \gamma_A) \rho_{eg} + iW(t) \sum_m \frac{g_m}{\sqrt{\varepsilon_0 E_{vac}^m}} a_m \quad (2)$$

where, ρ_{eg} is the dipole transition density matrix element, ω_A is the resonant angular frequency of the QEs, γ_A is the decay rate. $W(t)$ is the population difference function, g_m is the coupling

strength between a single QE and the m -th mode in plasmonic resonator, E_{vac}^m is the vacuum field of the m th mode. According to the Heisenberg operator equations [36] and multimode interference coupled mode theory (MICMT) [34], it can be obtained that

$$\begin{aligned} \frac{da_m}{dt} = & - \left(i\omega_m + \frac{1}{\tau_{m0}} + \frac{1}{\tau_{m1}} + \frac{1}{\tau_{m2}} \right) a_m \\ & - ig_m \sqrt{\varepsilon_0} E_{vac}^m \rho_{eg} \\ & + \kappa_{m1} b_{m,1+} + \kappa_{m2} b_{m,2+} \end{aligned} \quad (3)$$

$$b_{1-} = -b_{1+} + \sum_m \kappa_{m1}^* a_m \quad (4)$$

$$b_{2-} = -b_{2+} + \sum_m \kappa_{m2}^* a_m \quad (5)$$

where, $b_{i\pm} = \sum_m b_{m,i\pm}$ are the field amplitudes in each waveguide ($i = 1, 2$, for incoming (+) or outgoing (-) from the resonator), $\kappa_{m1} = e^{i\theta_{m1}} \sqrt{2/\tau_{m1}}$ and $\kappa_{m2} = e^{i\theta_{m2}} \sqrt{2/\tau_{m2}}$. In the weak excitation limit, QEs are basically in the ground state [36], which means $W(t) = -1$. The coupling strength between QEs and the resonant mode in plasmonic resonator is closely related to the field distribution. Fig. 2(a) and (b) show the distribution of the electric field components $|E_x|$ and $|E_y|$ at the resonant wavelength of 1390 nm, from which it can be found that the electric field energy of the $TM_{1,0}$ mode is mainly concentrated in the rectangular cavity, the energy in VG cavity is almost zero. Since the nanowire is placed in VG cavity, the coupling between QEs and $TM_{1,0}$ mode is approximately zero. We can ignore the coupling between the QEs and $TM_{1,0}$ mode, and only consider the coupling between QEs and the TM_v mode of which the resonant frequency is very close to that of the QEs. For symmetrical system $\tau_{m1} = \tau_{m2} = \tau_m$, the transmission coefficient expression of the hybrid system can be expressed as follows

$$\begin{aligned} t = & \sum_m \frac{2e^{i\varphi_1} (-i\Delta_A + \gamma_A)}{\left(-i\Delta_1\tau_1 + 2 + \frac{\tau_1}{\tau_{10}} \right) (-i\Delta_A + \gamma_A) + \tau_1 g_1^2} \\ & + \frac{2e^{i\varphi_2}}{-i\Delta_2\tau_2 + 2 + \frac{\tau_2}{\tau_{20}}} \end{aligned} \quad (6)$$

Here $\Delta_{A,1,2} = \omega - \omega_{A,1,2}$, $\varphi_1 = \theta_{11} - \theta_{12}$, $\varphi_2 = \theta_{21} - \theta_{22}$. Fig. 2(d) shows the simulation (blue) and theoretical (red) curves of the transmittance of the hybrid system with the nanowire in VG cavity embedded with QEs. Obvious mode splitting appears in the transmission spectrum, and the distance between the two split peaks (80 nm) in Fig. 2(d) is much larger than the full width at half maximum (FWHM) (42 nm) of the transmission window of TM_v mode in Fig. 2(c), which indicates that the coupling between QEs and the TM_v mode of VG cavity is strong coupling. By curve-fitting, the coupling and internal loss decay time of the TM_v mode can be obtained as $\tau_1 = 50$ fs and $\tau_{10} = 100$ fs, which will be used in the research of the non-weak excitation limit in next section.

IV. NON WEAK EXCITATION LIMIT

The above analysis and study is performed under the weak excitation limit the case of which the incident light intensity is very weak. As the incident light intensity is stronger, the QEs in the nanowire no longer remain in the ground state. This means the population difference operator $W(t)$ cannot be approximated as a constant -1 , but a function changing with time, and the transmission coefficient expression (6) is no longer applicable. In this case, the QEs in nanowire is described by Bloch equations

$$\frac{dW}{dt} = 2\Omega_R(t) [U \sin(\Delta_A t) - V \cos(\Delta_A t)] \quad (7)$$

$$\frac{dU}{dt} = -\frac{\Omega_R(t)}{2} W \sin(\Delta_A t) \quad (8)$$

$$\frac{dV}{dt} = \frac{\Omega_R(t)}{2} W \cos(\Delta_A t) \quad (9)$$

where, $\Omega_R(t) = -\boldsymbol{\mu} \cdot \boldsymbol{\psi}(\mathbf{r})|a(t)|/(\hbar\sqrt{\epsilon_0}) = \chi|a|$, μ is the transition dipole moment of a single QE (take 0.5 *enm* in this article), is the normalized distribution function of the electric field. (W, U, V) is Bloch vector, $W = \rho_{ee} - \rho_{gg}$, $V = (\rho_{eg} - \rho_{ge})/(2i)$. When the system is at resonance ($\Delta_A = 0$) and the initial condition is $W(0) = -1$, $V(0) = 0$, the solutions of the Bloch equations are

$$W(t) = -\cos\left(\int_0^t \Omega_R dt\right) \quad (10)$$

$$V(t) = -\frac{1}{2} \sin\left(\int_0^t \Omega_R dt\right) \quad (11)$$

If the mode volume of the TM_v mode in VG cavity is V_{eff} , the equivalent number density of QEs in the nanowire is $n = NV_{\text{eff}}$, then the output power density of the nanowire embedded with QEs is

$$p_{QE} = -n\hbar\omega_A \frac{1}{2} \frac{dW}{dt} = -n\hbar\omega_A (\Omega_R/2) \sin\left(\int_0^t \Omega_R dt\right) \quad (12)$$

Equation (12) shows that the coupling between QEs and the VG cavity will make the QEs system to absorb or release energy, this energy will be converted into the electromagnetic field energy in VG cavity. This is equivalent to adding an additional field a_{QE} , which is a stimulated radiation field and in phase with a_1 . Then, the total field in the VG cavity is $a = a_1 + a_{QE}$. Since the output power density of the QEs system induces an additional field a_{QE} , it is necessary to make the following corrections to the coupled mode theory (CMT) equation

$$\frac{da_1}{dt} = -\left(i\omega_1 + \frac{1}{\tau_{10}} + \frac{1}{\tau_{11}} + \frac{1}{\tau_{12}}\right) a_1 + \kappa_{11} b_{1+} + \kappa_{12} b_{2+} \quad (13)$$

$$b_{1-} = -b_{1+} + \kappa_{11}^* a \quad (14)$$

$$b_{2-} = -b_{2+} + \kappa_{12}^* a \quad (15)$$

For symmetrical systems, when the excitation light is resonated with the QEs and only injected from waveguide S_1 (that means

$b_{2+} = 0$), according to the power conservation

$$|b_{1+}|^2 + p_{QE} = |b_{1-}|^2 + |b_{2-}|^2 + \frac{2}{\tau_{10}} |a|^2 + \frac{d|a|^2}{dt} \quad (16)$$

Then, the following equation on the electric field amplitude can be obtained

$$\begin{aligned} \frac{d|a|}{dt} + \left(\frac{2}{\tau_1} + \frac{1}{\tau_{10}}\right) (|a| - |a_1|) \\ + \frac{\chi}{4} \sin\left(\int_0^t \Omega_R dt\right) n\hbar\omega_A = 0 \end{aligned} \quad (17)$$

At this time, the transmittance of the hybrid system can be expressed as

$$T = \left|\frac{b_{2-}}{b_{1+}}\right|^2 = T_0 \left|\frac{a(t)}{a_1}\right|^2 \quad (18)$$

T_0 is the transmittance of the system without QEs in nanowire.

Equation (18) shows that the transmittance of the hybrid system can be obtained as a function of time after solving the changing field amplitude $|a(t)|$ from (17). Moreover, the relationship between the field amplitude $|a_1|$ and the incident light intensity is $I_{in} = c|a_1|^2/(n_{\text{eff}}T_0)$, which indicates that the transmittance of the hybrid system is also related to the incident light intensity, c is the speed of light in free space, n_{eff} is the equivalent refractive index of the waveguide. Based on (17) and (18), next investigated will be the influences of the incident light intensity and the QEs number density on the transmittance function of the hybrid system in the case of continuous light input.

Since the transmittance of the hybrid system is oscillating with time, two important parameters to describe the oscillation will be studied — pulse repetition frequency (PRF) and extinction ratio [$EXT = 10\log_{10}(T_{\text{max}}/T_{\text{min}})$]. The pseudo-color diagrams of the dependence of PRF and EXT on the incident light intensity and the QEs number density are shown in Fig. 3(a) and (b). Firstly, the point B (170, 1.8) is taken as an example to elucidate the formation mechanism of the femtosecond pulses with high repetition frequency.

The curve of the transmittance changing with time under the condition of point B is shown in Fig. 3(c). According to the expression (12) of the output power density, the phase function is defined as $\varphi(t) = \int_0^t \Omega_R dt$. According to the phase function, a period can be divided into three stages. The duration from 0 to t_1 is called stage I. In stage I, $0 < \varphi < \pi$, then $p_{QE} < 0$. This indicates that the QEs are absorbing energy, the total field amplitude $|a| = |a_1| - |a_{QE}| < |a_1|$, and it is known that $T < T_0$ from the transmittance expression (15). The duration from t_1 to t_2 is called stage II. In stage II, $\pi < \varphi < 3\pi/2$, $p_{QE} > 0$. This indicates that the QEs are releasing energy, the total field amplitude $|a| = |a_1| + |a_{QE}| > |a_1|$, the transmittance of the system $T > T_0$. The duration from t_2 to t_3 is called stage III. Stage III is approximately the time mirror of stage II.

From 0 to t_3 is a pulse period. At the beginning, all QEs are in the ground state, due to the interaction between QEs and VG cavity, the QEs will absorb energy. Until the time of t_1 , all QEs have transitioned to the excited state, the process of the QEs

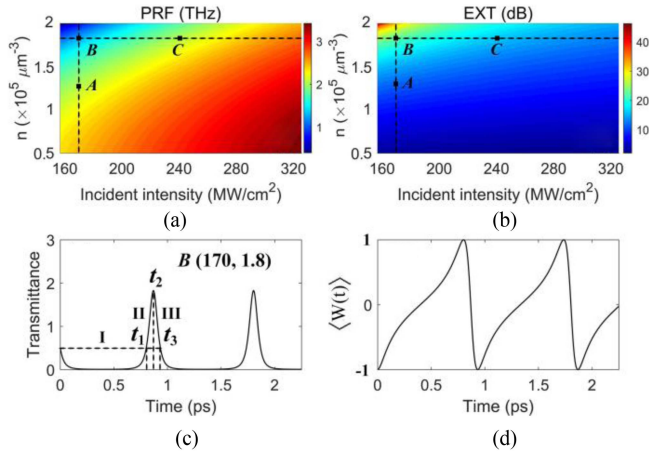


Fig. 3. (a) and (b) Pseudo-color diagrams of the dependence of PRF and EXT on the incident light intensity and the QEs number density. (c) and (d) Time evolution curves of the transmittance and the population difference function $W(t)$ at point B. The equivalent refractive index of the waveguide is $n_{\text{eff}} = 1.32$, initial transmittance is $T_0 = 0.5$. The nanowire is placed at the position of $\psi(r) = 1$.

system absorbing energy is over. After that, also attribute to the interaction between QEs and VG cavity, in stages II and III the QEs releases the energy absorbed in stage I. The field amplitude in the plasmonic resonator will be caused to oscillate with time by such a process of absorbing and releasing energy. Moreover, during the whole process of stage I, the total field amplitude in plasmonic resonator is smaller than that in stages II and III. And it can be known combined with the integral expression of the phase function that the duration of stage I is naturally longer than the total durations of stages II and III, as shown in Fig. 3(c). The collective population difference function can also be affected by the oscillating field amplitude, of which the time evolution curve is given by Fig. 3(d). Since the total field amplitude in stage I is relatively small, the rate of QEs transition from the ground state to the excited state is relatively slow, so the duration is relatively long. In stages II and III, the total field amplitude in plasmonic resonator is larger, the rate of QEs transition from the excited state to the ground state is faster, thereby the duration is shorter. This results in the transmittance of the system to behave as the form of pulse oscillation with time. The PRF and EXT of the pulse in Fig. 3(c) are 1.07 THz and 26 dB respectively, and the pulse width is 88 fs. When the QEs number density is constant, the smaller the incident light intensity, the longer the pulse period will become, and the closer it will be to the breathing pulse which can give rise to dense radio-frequency combs. And recently, Wu et al. [37] present the first in-depth study of the locking of breather oscillations to the cavity repetition frequency in a fibre laser. Be different from them, we realize the time-domain shaping of continuous waves by changing the intensity of incident light and the QEs number density, which provides another route to obtain femtosecond pulses with high repetition frequency at the nanoscale.

The pseudo-color images of Fig. 3(a) and (b) show that the PRF and EXT of the pulse oscillation are closely related to the incident light intensity and the QEs number density. Next, the

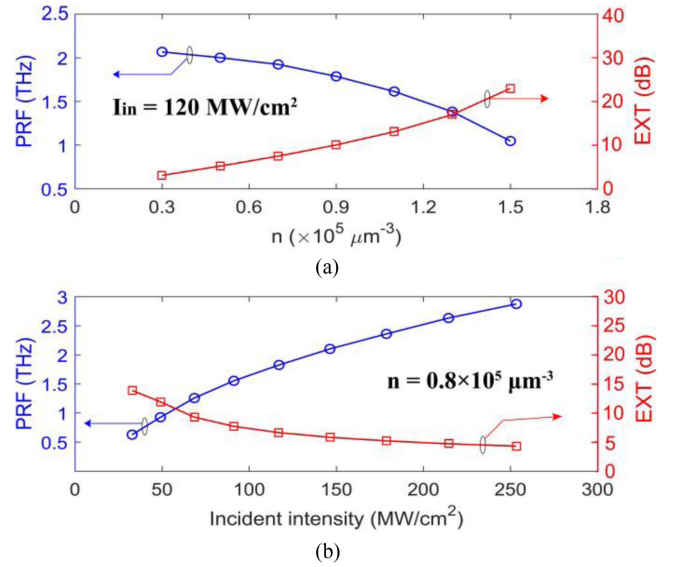


Fig. 4. (a) Curves of the PRF and EXT changing with the QEs number density when the incident light intensity is 120 MW/cm², respectively. (b) Curves of the PRF and EXT changing with the incident light intensity when the QEs number density is $0.8 \times 10^5 \mu\text{m}^{-3}$, respectively.

influence of the incident light intensity and the QEs number density on the PRF and EXT of the hybrid system will be studied respectively.

First studied is the influence of the QEs number density on PRF and EXT when the incident light intensity is constant. As shown in Fig. 4(a), when the incident light intensity is 120 MW/cm², the larger the QEs number density, the smaller the PRF and the larger the EXT. When the incident light intensity is constant, the larger the QEs number density, the greater the absorbed power of the QEs system in stage I, resulting in smaller total field amplitude in the resonator, and the duration of stage I will be longer. However, the time changes of stage II and III are much smaller than that of stage I. Overall, the time of a pulse period will become longer and the PRF will decrease. For extinction ratio, the larger the QEs number density, the smaller the minimum value of the total field amplitude in stage I, and the greater the output power density of the QEs system in stages II and III which results in greater total field amplitude at t_2 , so the EXT will increase. When the QEs number density is close to 0, the output power of the QEs system will also approach 0, the field amplitude in the resonator tends to the constant $|a_1|$, so the EXT will approach zero and the PRF tends to a limit value $\chi|a_1|/(2\pi)$.

Next analyzed is the influence of the incident light intensity on PRF and EXT when the QEs number density is fixed. As shown in Fig. 4(b), when the QEs number density is $n = 0.8 \times 10^5 \mu\text{m}^{-3}$, the PRF will increase but the EXT will decrease with the increase of the incident light intensity. When the QEs number density is constant, the stronger the incident light intensity, the greater the total field amplitude in all three stages, and the shorter the time for the phase to change from 0 to 2π , and thus the PRF will increase. From (12) and (15), it can be known that the ratio of the output power of the QEs system

to the transmission power is inversely proportional to the total field amplitude in VG cavity, that is $p_{QE}/|b_{2-}|^2 \propto 1/|a(t)|$. So, the larger the total field amplitude $|a(t)|$, the smaller the ratio $p_{QE}/|b_{2-}|^2$, which indicates that the stronger the incident light intensity, the weaker the influence of the QEs system on the transmission response, and the smaller the peak-to-valley ratio of the transmittance curve, naturally the EXT will decrease. When the incident light intensity is extremely strong, the influence of the QEs system on the transmission response of the hybrid system can be ignored, the transmittance of the system becomes the constant T_0 , and the PRF and EXT respectively tend to $\chi|a_1|/(2\pi)$ and 0.

Briefly, due to the interaction between the QEs and the field in VG cavity, Rabi oscillation occurs in QEs which result in the field amplitude in the resonant cavity also behave as the form of oscillation. In this way, the output power of the resonant cavity also exhibit as the form of pulse oscillation. The process of Rabi oscillation is closely related to incident light intensity and QEs number density. Rabi oscillation can be controlled by changing the incident light intensity and QEs number density, and then the repetition frequency and duration of the pulse oscillation output from the resonant cavity can be controlled. In other words, the pulse repetition frequency can be affected by the incident light intensity and QEs number density. When the QEs number density is constant, the greater the incident light intensity is, the higher the pulse repetition frequency will be. As the incident light intensity is constant, the higher the QEs number density is, the lower the pulse repetition frequency will be. Therefore, the pulse repetition frequency can be controlled by changing the incident light intensity and QEs number density.

Next, the influence of incident light intensity and QEs number density on pulse duration will be discussed. The dependence of the pulse duration on incident light intensity and QEs number density is shown in Fig. 5(a). Line AB and line BC are selected to study the changing trends of the pulse duration, respectively. When QEs number density is $n = 1.7 \times 10^5 \mu\text{m}^{-3}$, the pulse duration will decrease from 82.5 fs to 34 fs with the increase of the incident light intensity 157 MW/cm^2 to 357 MW/cm^2 . When the incident light intensity is 170 MW/cm^2 , the pulse duration will increase from 40.5 fs to 83 fs with the increase of the QEs number density from $0.3 \times 10^5 \mu\text{m}^{-3}$ to $1.8 \times 10^5 \mu\text{m}^{-3}$. Under the conditions shown in Fig. 5(a), the durations of the pulses are all less than 100 fs. Therefore, the pulse duration can be controlled by changing the incident light intensity and QEs Number density. Moreover, the optical spectrum of the output pulses under three different conditions of A (170, 0.5), B (170, 1.7), and C (350, 1.7) given in Fig. 5(a) are shown in Fig. 5(d)–(f). By comparing Fig. 5(d) and (e), it can be found that when the incident light intensity is constant, the greater the QEs number density is, the denser the optical spectrum of the pulses will be. By comparing Fig. 5(e) and (f), it can be found that when the QEs number density is constant, the larger the incident light intensity is, the sparser the optical spectrum of the pulses will be. The pulse duration at points A and C is smaller than that at point B, but the spectrum at point B is denser than both of them. The reason is that the PRF at point B is smaller than that at points A and C, while the EXT at point B is also much larger

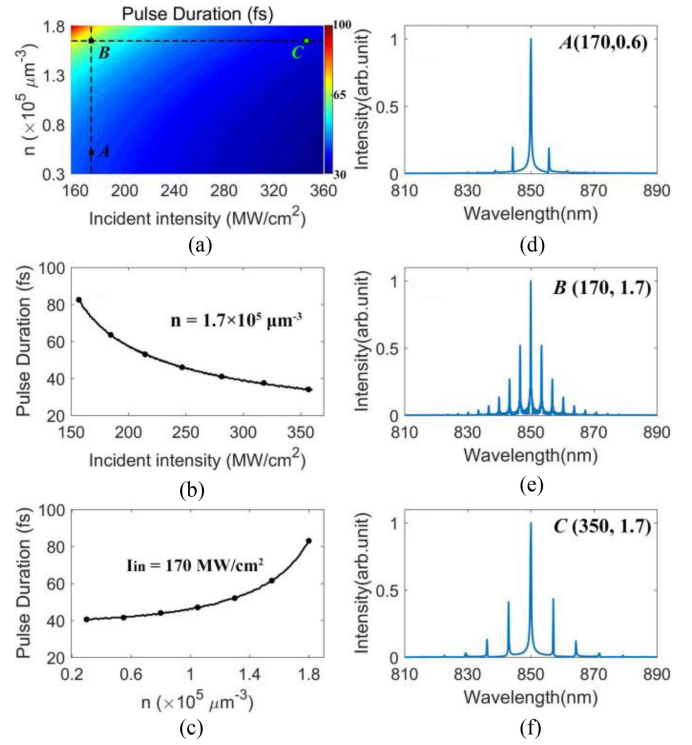


Fig. 5. (a) Pseudo-color diagrams of the dependence of pulse duration on the incident light intensity and the QEs number density. (b) Curves of the pulse duration changing with the incident light intensity when the QEs number density is $1.7 \times 10^5 \mu\text{m}^{-3}$. (c) Curves of the pulse duration changing with the QEs number density when the incident light intensity is 170 MW/cm^2 . (d)–(f) The optical spectrum of the output pulses under three different conditions A(170,0.5), B(170,1.7), C(350,1.7) shown in (a).

than that at points A and C. Therefore, the ratio of incident light intensity to QEs Number density should be as small as possible to obtain denser optical spectrum.

V. CONCLUSION

In summary, we studied the transmission response of a hybrid system consisting of plasmonic resonator and a nanowire embedded with two-level QEs. Investigations under the weak excitation limit show that the coupling between QEs and the TM_v mode of the VG cavity can reach the region of strong coupling. In the case of continuous wave incidence, attribute to the presence of QEs, the transmittance of the hybrid system behave as the form of pulse oscillation with time. The pulse repetition frequency could reach the magnitude of terahertz, simultaneously, the pulse width is below 100 fs and the extinction ratio also reaches very high values. Furthermore, we can freely control the pulse repetition frequency and extinction ratio by the incident light intensity and QEs number density to obtain the pulse oscillation required. Moreover, we also discussed the duration and spectral characteristics of the pulses. The pulse duration and spectral distribution can also be controlled by adjusting the incident light intensity and QEs number density. This provides a feasible route for achieving ultra-short pulses with high repetition frequency at the nanoscale, which also has potential applications in optical clock signals.

REFERENCES

- [1] D. J. Bergman and M. I. Stockman, "Surface plasmon amplification by stimulated emission of radiation: Quantum generation of coherent surface plasmons in nanosystems," *Phys. Rev. Lett.*, vol. 90, no. 2, Jan. 2003, Art. no. 027402.
- [2] A. H. Chin, S. Vaddiraju, A. V. Maslov, C. Z. Ning, M. K. Sunkara, and M. Meyyappan, "Near-infrared semiconductor subwavelength-wire lasers," *Appl. Phys. Lett.*, vol. 95, no. 20, 2006, Art. no. 163115.
- [3] R. Perahia, T. P. Mayer Alegre, A. Safavi-Naeini, and O. Painter, "Surface-plasmon mode hybridization in subwavelength microdisk lasers," *Appl. Phys. Lett.*, vol. 88, no. 16, 2009, Art. no. 201114.
- [4] S. W. Eaton, A. Fu, A. B. Wong, C. Z. Ning, and P. Yang, "Semiconductor nanowire lasers," *Nature Rev. Mater.*, vol. 1, no. 6, pp. 1–11, May 2016.
- [5] O. Painter et al., "Two-dimensional photonic band-gap defect mode laser," *Science*, vol. 284, no. 5421, pp. 1819–1821, Jun. 1999.
- [6] S. I. Azzam et al., "Ten years of spasers and plasmonic nanolasers," *Light Sci. Appl.*, vol. 9, no. 1, 2020, Art. no. 90.
- [7] R. F. Oulton et al., "Plasmon lasers at deep subwavelength scale," *Nature*, vol. 461, no. 7264, pp. 629–632, Aug. 2009.
- [8] W. Zhu et al., "Surface plasmon polariton laser based on a metallic trench Fabry-Perot resonator," *Sci. Adv.*, vol. 3, no. 10, 2017, Art. no. e1700909.
- [9] E. K. Keshmariz, R. N. Tait, and P. Berini, "Single-mode surface plasmon distributed feedback lasers," *Nanoscale*, vol. 10, no. 13, pp. 5914–5922, Feb. 2018.
- [10] W. L. Barnes, A. Dereux, and T. W. Ebbesen, "Surface plasmon subwavelength optics," *Nature*, vol. 424, no. 6950, pp. 824–830, Aug. 2003.
- [11] A. D. Jameson et al., "Direct measurement of light-matter energy exchange inside a microcavity," *Optica*, vol. 1, no. 5, pp. 276–280, Oct. 2014.
- [12] K. Santhosh, O. Bitton, L. Chuntonov, and G. Haran, "Vacuum Rabi splitting in a plasmonic cavity at the single quantum emitter limit," *Nature Commun.*, vol. 7, no. 1, pp. 1–5, Jun. 2016.
- [13] P. Vasa et al., "Coherent exciton-surface plasmon polariton interactions in hybrid metal semiconductor nanostructures," *Phys. Rev. Lett.*, vol. 101, no. 11, 2008, Art. no. 116801.
- [14] G. Zengin, M. Wersäll, S. Nilsson, T. J. Antosiewicz, M. Käll, and T. Shegai, "Realizing strong light-matter interactions between single-nanoparticle plasmons and molecular excitons at ambient conditions," *Phys. Rev. Lett.*, vol. 114, no. 15, 2015, Art. no. 157401.
- [15] T. B. Hoang, G. M. Akselrod, and M. H. Mikkelsen, "Ultrafast room-temperature single photon emission from quantum dots coupled to plasmonic nanocavities," *Nano Lett.*, vol. 16, no. 1, pp. 270–275, Nov. 2015.
- [16] S. Balci, B. Kucukoz, O. Balci, A. Karatay, C. Kocabas, and G. Yaglioglu, "Tunable Plexcitonic nanoparticles: A model system for studying plasmon-exciton interaction from weak to ultrastrong coupling regime," *Amer. Chem. Soc. Photon.*, vol. 3, no. 11, pp. 2010–2016, Oct. 2016.
- [17] J. Bellessa, C. Bonnard, J. C. Plenet, and J. Mugnier, "Strong coupling between surface plasmons and excitons in an organic semiconductor," *Phys. Rev. Lett.*, vol. 93, no. 3, 2004, Art. no. 036404.
- [18] R. Chikkaraddy et al., "Single-molecule strong coupling at room temperature in plasmonic nanocavities," *Nature*, vol. 535, no. 7610, pp. 127–130, Jun. 2016.
- [19] P. Vasa et al., "Real-time observation of ultrafast Rabi oscillations between excitons and plasmons in metal nanostructures with J-aggregates," *Nature Photon.*, vol. 7, no. 2, pp. 128–132, Jan. 2013.
- [20] A. Demetriadou, J. M. Hamm, Y. Luo, J. B. Pendry, J. J. Baumberg, and O. Hess, "Spatiotemporal dynamics and control of strong coupling in plasmonic nanocavities," *Amer. Chem. Soc. Photon.*, vol. 4, no. 10, pp. 2410–2418, Sep. 2017.
- [21] R. Liu et al., "Strong light-matter interactions in single open plasmonic nanocavities at the quantum optics limit," *Phys. Rev. Lett.*, vol. 118, no. 23, 2017, Art. no. 237401.
- [22] J. Ren, Y. Gu, D. Zhao, F. Zhang, T. Zhang, and Q. Gong, "Evanescence-enhanced photon-exciton coupling and fluorescence collection," *Phys. Rev. Lett.*, vol. 118, no. 7, 2017, Art. no. 073604.
- [23] J. O'Brien, B. Patton, M. Sasaki, and J. Vučković, "Focus on integrated quantum optics," *New J. Phys.*, vol. 15, no. 3, 2013, Art. no. 035016.
- [24] M. K. Kim, A. M. Lakhani, and M. C. Wu, "Efficient waveguide-coupling of metal-clad nanolaser cavities," *Opt. Exp.*, vol. 19, no. 23, pp. 23504–23512, Nov. 2011.
- [25] R. M. Ma, X. Yin, R. F. Oulton, V. J. Sorger, and X. Zhang, "Multiplexed and electrically modulated plasmon laser circuit," *Nano Lett.*, vol. 12, no. 10, pp. 5396–5402, Sep. 2012.
- [26] V. Dolores-Calzadilla et al., "Waveguide-coupled nanopillar metal-cavity light emitting diodes on silicon," *Nature Commun.*, vol. 8, no. 1, 2017, Art. no. 14323.
- [27] C. Z. Ning, "Semiconductor nanolasers and the size-energy-efficiency challenge: A review," *Adv. Photon.*, vol. 1, no. 1, 2019, Art. no. 014002.
- [28] R. M. Ma, S. Ota, Y. Li, S. Yang, and X. Zhang, "Explosives detection in a lasing plasmon nanocavity," *Nature Nanotechnol.*, vol. 9, no. 8, pp. 600–604, Jul. 2014.
- [29] S. Wang et al., "High-yield plasmonic nanolasers with superior stability for sensing in aqueous solution," *Amer. Chem. Soc. Photon.*, vol. 4, no. 6, pp. 1355–1360, May 2017.
- [30] X. Y. Wang et al., "Lasing enhanced surface plasmon resonance sensing," *Nanophotonics*, vol. 6, no. 2, pp. 472–478, Feb. 2017.
- [31] P. J. Cheng et al., "High-performance plasmonic nanolasers with a nanotrench defect cavity for sensing applications," *Amer. Chem. Soc. Photon.*, vol. 5, no. 7, pp. 2638–2644, Mar. 2018.
- [32] S. Li, Y. Ding, R. Jiao, G. Duan, and L. Yu, "Femtosecond pulse with THz repetition frequency based on the coupling between quantum emitters and a plasmonic resonator," *Phys. Rev. A*, vol. 97, Mar. 2018, Art. no. 033811.
- [33] K. E. Oughstun and N. A. Cartwright, "On the Lorentz-Lorenz formula and the Lorentz model of dielectric dispersion," *Opt. Exp.*, vol. 11, no. 13, pp. 1541–1546, Jun. 2003.
- [34] S. Li, Y. Wang, R. Jiao, L. Wang, G. Duan, and L. Yu, "Fano resonances based on multimode and degenerate mode interference in plasmonic resonator system," *Opt. Exp.*, vol. 25, no. 4, pp. 3525–3533, Feb. 2017.
- [35] J. Chen, C. Sun, and Q. Gong, "Fano resonances in a single defect nanocavity coupled with a plasmonic waveguide," *Opt. Lett.*, vol. 39, no. 1, pp. 52–55, Dec. 2014.
- [36] E. Waks and J. Vučković, "Dipole induced transparency in drop-filter cavity-waveguide systems," *Phys. Rev. Lett.*, vol. 96, no. 15, 2006, Art. no. 153601.
- [37] X. Wu, Y. Zhang, J. G. Peng, S. Boscolo, C. Finot, and H. Zeng, "Farey tree and devil's staircase of frequency locked breathers in ultrafast lasers," *Nature Commun.*, vol. 13, no. 5784, pp. 1–10, Oct. 2022.